

Intermediate-spin state and properties of LaCoO_3

M. A. Korotin, S. Yu. Ezhov, I. V. Solovyev, and V. I. Anisimov
Institute of Metal Physics, Russian Academy of Sciences, 620219 Yekaterinburg GSP-170, Russia

D. I. Khomskii* and G. A. Sawatzky

Solid State Physics Laboratory, University of Groningen, Nijenborg 4, 9747 AG Groningen, The Netherlands

(Received 6 November 1995)

The electronic structure of the perovskite LaCoO_3 for different spin states of Co ions was calculated in the local-density approximation LDA+ U approach. The ground state is found to be a nonmagnetic insulator with Co ions in a low-spin state. Somewhat higher in energy, we find two intermediate-spin states followed by a high-spin state at significantly higher energy. The calculations show that Co 3d states of t_{2g} symmetry form narrow bands which could easily localize, while e_g orbitals, due to their strong hybridization with the oxygen 2p states, form a broad σ^* band. With temperature variation which is simulated by a corresponding change of the lattice parameters, a transition from the low- to intermediate-spin state occurs. This intermediate-spin (occupation $t_{2g}^5 e_g^1$) can develop an orbital ordering which can account for the nonmetallic nature of LaCoO_3 at 90 K $< T < 500$ K. Possible explanations of the magnetic behavior and gradual insulator-metal transition are suggested. [S0163-1829(96)07632-1]

I. INTRODUCTION

Among the systems showing a semiconductor-to-metal transition, LaCoO_3 is especially interesting because of its very unusual magnetic behavior, often associated with a low-spin (LS)–high-spin (HS) transition.¹ Although a large number of investigations have been carried out since the early 1960s, the character of the transition and the nature of the temperature dependence of the spin state is still unclear. For example, the temperature dependence of the magnetic susceptibility shows a strong maximum at around 90 K followed by a Curie-Weiss-like decrease at higher temperatures,² which was interpreted by the authors as a LS-to-HS transition. The semiconductor to metal-like transition occurs in a range of 400–600 K, well above this transition. The insulating nature of LaCoO_3 below 400–600 K was attributed by Raccach and Goodenough to an ordering of LS and HS Co^{3+} ions in a NaCl-like structure,¹ with the itinerant electrons in a broadband formed by the transition-metal e_g orbitals. This structural change, however, has not been observed in crystallographic studies. Recent neutron-scattering experiments³ suggest that the semiconductor-metal transition is not predominantly magnetic in origin, but a clear picture of its nature is absent.

X-ray photoemission (XPS) and x-ray-absorption (XAS) studies, on the other hand, have been interpreted in terms of a spin change at the semiconductor-metal transition.⁴ There are, however, several discrepancies in the interpretation. The Co 2p XAS line shape at room temperature looks like LS Co^{3+} , which is not consistent with a spin state transition at 90 K. Also, the valence-band XPS spectrum at 300 K is quite different from that of a HS compound. So the interpretation of the two transitions is still uncertain.

In most previous studies one has assumed a rather ionic and ligand-field-like starting point. In this picture the possibility of intermediate-spin (IS) states as well as local symmetry lowering, orbital ordering, and the large bandwidth of

the e_g states, were not considered. It has recently been pointed out by several authors that the oxides corresponding to high formal oxidation states may be negative charge-transfer systems in the Zaanen-Sawatzky-Allen scheme,⁵ resulting in an essential modification of the electronic structure, in particular in a possible stabilization of an IS state.⁶

A first physical model to explain the transitions in LaCoO_3 was proposed and recently revised by Goodenough in Ref. 1. It was suggested that for trivalent cobalt in LaCoO_3 the crystal-field energy Δ_{cf} is only slightly larger than the intraatomic (Hund) exchange energy Δ_{ex} . Thus the ground state of the Co ion is LS 1A_1 ($S=0$), and the excited HS state 5T_2 ($S=2$), according to Ref. 1, is only 0.08 eV higher in energy. The corresponding one-electron configurations are $t_{2g}^6 e_g^0$ for the LS state and $t_{2g}^4 e_g^2$ for the HS state. The increase in temperature leads to the population of the HS states which is reflected in the magnetic susceptibility measurements. The semiconductor-metal transition was interpreted qualitatively as a formation of a σ^* band from the localized ionic e_g states. The long-range order of the LS and HS Co ions was assumed based on the results of x-ray-diffraction measurements. Recent neutron-diffraction experiments³ did not confirm this, but also did not exclude possible short-range order of this kind.

The theoretical description of LaCoO_3 is a difficult task, because this system exhibits a transition from localized to delocalized behavior, and the two main existing methods— one-electron band-structure calculations based on the local-density-approximation (LDA) and “model Hamiltonian configuration interaction” approaches (which were both used for the compound under consideration^{4,7})—were constructed for the completely itinerant and fully localized cases, respectively.

Recently Sarma *et al.*⁸ presented results of the local spin density approximation (LSDA) calculations for LaMO_3 ($M = \text{Mn, Fe, Co, Ni}$). It was claimed there that LSDA results gave good agreement with the x-ray photoemission spectra.

Such an agreement is not necessarily proof of an adequate description of the electronic structure. A well-known example is NiO, where LSDA gives a sharp peak at the top of the valence band in agreement with XPS, but the nature of this peak is the Ni $3d t_{2g}$ minority spin, while it is generally accepted that this peak is derived from the d^8L final state. The real proof of the correctness of the one-electron approximation would be an absence of the satellites in the photoemission spectra. Also, the XPS spectra, with which a comparison was made in Ref. 8, were measured at room temperature, where LaCoO_3 is already not in the low-spin state. So these XPS data must be compared with LSDA results corresponding to the magnetic solution and not to a nonmagnetic one as in Ref. 8.

Anisimov, Zaanen, and Andersen proposed a so-called LDA+ U method⁹ which combines in one calculation scheme LDA and Hubbard model approaches, and is able to treat on a ‘‘first-principle’’ basis systems with a strong Coulomb correlation. It was demonstrated that this method (in contrast to the standard LDA) could describe the existence of different states of the system under consideration which are close in total energy (holes in doped copper oxides¹⁰ and transition-metal impurities in insulators¹¹).

In this paper we present a study of the electronic structure of LaCoO_3 in the LDA+ U approach. In contrast to the standard LDA there are several stable solutions corresponding to different local minima of the LDA+ U functional. We have found a nonmagnetic insulating ground state in agreement with experiment. We have also found two orbitally polarized magnetic solutions corresponding to IS states (one of them is a gapless semiconductor and the other is a metal) and a semi-conducting magnetic solution corresponding to a HS state of the system, which lies much higher in energy. In addition we found that the e_g states form broadbands, whereas the t_{2g} states exhibit narrow bands, split by Coulomb interactions into lower (occupied) and upper (unoccupied) Hubbard bands. Using the results of these calculations, we propose an interpretation of the behavior of LaCoO_3 . According to our scheme, with increasing temperature there first occurs a transition from a LS (nonmagnetic) insulating ground state to a state with an IS (configuration $t_{2g}^5 e_g^1$). Due to the strong Jahn-Teller nature of this configuration, this state may develop orbital ordering. The orbitally ordered state turns out to be nonmetallic (actually nearly a zero-gap semiconductor) in our calculations. With a further increase of temperature the orbital ordering may be gradually destroyed, which can explain the transition to a metallic state observed in LaCoO_3 at 400–600 K. We hope that this information will eventually lead to a better understanding of LaCoO_3 and other similar materials.

II. CALCULATION METHOD

The LDA+ U method⁹ is based on the assumption that it is possible to separate all electrons in the system into two subsets: the localized states (for LaCoO_3 these are the Co $3d$ orbitals), for which Coulomb intrashell interactions are described by the Hubbard-like term, and the itinerant states, where the averaged LDA energy and potentials are good approximations.

It is known that LDA calculations can provide all the

necessary model parameters (such as the Coulomb parameter U ,¹² the exchange J , hopping parameters describing hybridization, etc.) on a first-principle basis, but the one-electron structure of the LDA equations with an orbital-independent potential does not allow to use these parameters in the full variational space. LDA+ U overcomes this problem by using the framework of the degenerate Anderson model in the mean-field approximation. In this method, the trial function is chosen as a single Slater determinant, so it is still a one-electron method, but the potential becomes occupation dependent, and that allows one to reproduce the main feature of strongly correlated systems: the splitting of the d band to the occupied lower Hubbard band and unoccupied upper Hubbard band.

The main idea of our LDA+ U method is that the LDA gives a good approximation for the average Coulomb energy of d - d interactions E_{av} as a function of the total number of d electrons $N = \sum_{m\sigma} n_{m\sigma}$, where $n_{m\sigma}$ is the occupancy of a particular $d_{m\sigma}$ orbital:

$$E_{av} = U \frac{N(N-1)}{2} - J \frac{N(N-2)}{4}. \quad (1)$$

But the LDA does not properly describe the full Coulomb and exchange interactions between d electrons in the same d shell. So we suggest subtracting E_{av} from the LDA total-energy functional, and adding orbital- and spin-dependent contributions to obtain the exact (in the mean-field approximation) formula

$$\begin{aligned} E = E_{\text{LDA}} - & \left(U \frac{N(N-1)}{2} - J \frac{N(N-2)}{4} \right) \\ & + \frac{1}{2} \sum_{m,m',\sigma} U_{mm'} n_{m\sigma} n_{m'-\sigma} \\ & + \frac{1}{2} \sum_{m \neq m', m', \sigma} (U_{mm'} - J_{mm'}) n_{m\sigma} n_{m'\sigma}. \end{aligned} \quad (2)$$

The derivative of Eq. (2) with orbital occupancy $n_{m\sigma}$ gives the expression for the occupation-dependent one-electron potential:

$$\begin{aligned} V_{m\sigma}(\mathbf{r}) = & V_{\text{LDA}}(\mathbf{r}) + \sum_{m'} (U_{mm'} - U_{\text{eff}}) n_{m'-\sigma} \\ & + \sum_{m' \neq m} (U_{mm'} - J_{mm'} - U_{\text{eff}}) n_{m\sigma} \\ & + U_{\text{eff}} \left(\frac{1}{2} - n_{m\sigma} \right) - \frac{1}{4} J. \end{aligned} \quad (3)$$

The Coulomb and exchange matrices $U_{mm'}$ and $J_{mm'}$ are

$$U_{mm'} = \sum_k a_k F^k, \quad (4)$$

$$J_{mm'} = \sum_k b_k F^k, \quad (5)$$

$$a_k = \frac{4\pi}{2k+1} \sum_{q=-k}^k \langle lm | Y_{kq} | lm \rangle \langle m' | Y_{kq}^* | lm' \rangle, \quad (6)$$

TABLE I. Basis set and MT-sphere radii used in the calculation.

Atom	$\kappa_1^2 = -0.01$ Ry	$\kappa_2^2 = -1.0$ Ry	$\kappa_3^2 = -2.3$ Ry	$R_{\text{MT}}, \text{\AA}$
La	6s6p5d4f	6s6p5d4f	6s6p5d	1.77
Co	4s4p3d	4s4p3d	4s4p	1.26
O	2s2p	2s2p	2s	0.66

$$b_k = \frac{4\pi}{2k+1} \sum_{q=-k}^k |\langle lm|Y_{kq}|lm'\rangle|^2, \quad (7)$$

where F^k 's Slater integrals and $\langle lm|Y_{kq}|lm'\rangle$ are integrals over products of three spherical harmonics Y_{lm} .

For d electrons, one needs F^0 , F^2 , and F^4 , and these can be linked to the parameters U (direct Coulomb interaction) and J (intraatomic exchange) obtained from the LSDA supercell procedures¹² via $U = F^0$ and $J = (F^2 + F^4)/14$, while the ratio F^2/F^4 is to a good accuracy constant ~ 0.625 for 3d elements.¹³ For LaCoO₃ the Coulomb parameter U was found to be 7.8 eV and the exchange parameter $J = 0.92$ eV.

The LDA+ U approximation was applied to the full potential linearized muffin-tin orbital (FP LMTO) calculation scheme.¹⁴ Crystallographic data being used in the calculations were taken from Ref. 3. According to them, LaCoO₃ has a pseudocubic perovskite structure with a rhombohedral distortion along the (111) direction. The unit cell contains two formula units. Since this rhombohedral distortion is small (the largest rhombohedral angle is 60.990° at 4 K), we use the concept of t_{2g} and e_g orbitals, as referred to in the cubic setting in the following discussion. Temperature was introduced in our calculations only by the change of lattice parameter and rhombohedral angle according to the data of Ref. 3. The most detailed description of the technical aspects of FP LMTO calculations for the perovskite-type complex oxides can be found in Ref. 15. The optimal choice of the basis set for describing the valence band and the bottom of the conduction band of LaCoO₃ is presented in Table I. Since the U correction is applied to the Co d orbitals, the value of the *muffin-tin* (MT) radius for Co was chosen close to its value in metallic Co in order to obtain the full 3d density inside the sphere. For the correct description of the wave functions in the interstitial region, we expanded the spherical harmonics up to the value of $l_{\text{max}} = 5, 4, \text{ and } 3$ for La, Co, and O MT spheres correspondingly. The Brillouin-zone (BZ) in-

tegration in the course of the self-consistency iterations was performed over a mesh of 65 \mathbf{k} points in the irreducible part of the BZ. Densities of states were calculated by the tetrahedron method with 729 \mathbf{k} points in the whole BZ.

As the potentials for the various d orbitals of Co are different in LDA+ U , it is not obvious *a priori* what will be the final symmetry of the system under consideration. In preliminary calculations we assumed for simplicity that LaCoO₃ has a perfect perovskite-type cubic lattice. To allow the system to choose the appropriate symmetry by itself, we perform an integration not over $\frac{1}{48}$ part of the BZ as for cubic symmetry but over $\frac{1}{8}$ (D_{2h} symmetry group). The resulting symmetries were found to be cubic O_h for the ground (LS) state and tetragonal D_{4h} for the excited states. Practically the same situation occurs in real $R\bar{3}c$ symmetry: the occupancies of xy , yz , and zx orbitals are about the same for the low-spin configuration as well as that of $3z^2-r^2$ and x^2-y^2 orbitals. The degeneracy of xy and yz and zx orbitals is broken in the other spin states.

III. RESULTS AND DISCUSSION

A. Homogeneous solutions

We start by considering the results of the calculations for the homogeneous regimes, without an extra superstructure. The possibility of obtaining a solution with orbital ordering is considered in Sec. III B.

The detailed results of the calculations with crystallographic data corresponding to 4 K are presented in Table II. One must start with equal occupancies of all three t_{2g} orbitals and also of two e_g orbitals (e.g., $t_{2g}^6 e_g^0$) to obtain the LS configuration. The initial spin polarization vanished during self-consistency iterations, resulting in a nonmagnetic final solution. The charge excitation spectrum has a semiconducting character in accordance with experimental data¹⁶ (and in contrast to the LDA result⁷) with the energy gap equal to 2.06 eV. The top of the valence band (Fig. 1) is formed by the mixture of oxygen 2p states with Co t_{2g} orbitals, and the bottom of the conduction band predominantly by the e_g orbitals.

From x-ray photoemission and absorption spectra⁴ the gap was estimated to be 0.9 ± 0.3 eV. The optical measurements¹⁷ gave ≈ 0.5 eV. The larger value of the calculated gap can be explained by the well-known fact that a mean-

TABLE II. Total-energy difference, character of the energy spectrum, occupancies of various d orbitals of Co, and magnetic moments for various Co spin states in LaCoO₃.

Configuration	δ^a (eV)	Energy gap (eV)	d occupancies						$\mu_{d\text{-Co}}$ (μ_B)	
			xy	yz	zx	$3z^2-r^2$	x^2-y^2	total		
$t_{2g}^6 e_g^0$ low spin		2.06	\uparrow, \downarrow	0.98	0.98	0.99	0.32	0.33	7.20	0
$t_{2g}^5 \sigma^*$ intermediate spin	0.24	0 ^b	\uparrow \downarrow	0.98 0.07	0.98 0.98	0.98 0.99	0.84 0.23	0.84 0.24	7.13	2.11
$t_{2g}^4 e_g^2$ high spin	0.65	0.13	\uparrow \downarrow	0.99 0.99	0.99 0.08	0.99 0.11	1.00 0.33	1.00 0.30	6.78	3.16

^aTotal-energy difference relative to the energy of $t_{2g}^6 e_g^0$ configuration.

^bHalf-metal. Total magnetic moment per unit cell is $2\mu_B$.

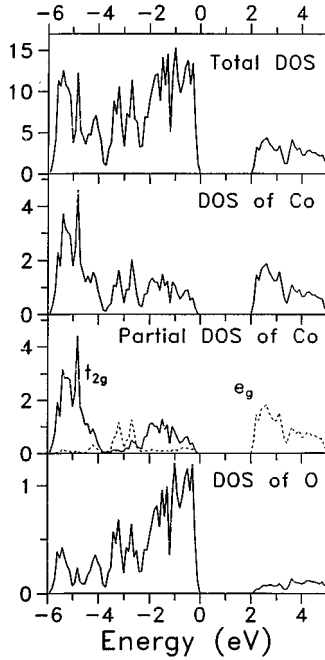


FIG. 1. The total (in states/eV cell) and partial (in states/eV atom) densities of states obtained in LDA+ U calculations for LaCoO₃ with Co ions in the low-spin state ($t_{2g}^6 e_g^0$ configuration). For the d -Co partial density of states, the solid line denotes t_{2g} orbitals, and the dashed line an e_g orbital.

field approximation, which is the basis of our LDA+ U approach, usually overestimates the tendency to localization and hence the values of the gap.

The aim of our work was to find solutions corresponding to the higher-spin states of Co ions. Usually the HS state is described as a $t_{2g}^4 e_g^2$ configuration with the maximum value of spin $S=2$ (magnetic moment $\mu_{Co}=4\mu_B$). This corresponds to the purely ionic model, and hybridization of the Co $3d$ orbitals with the oxygen $2p$ orbitals and band formation in a solid can renormalize significantly this ionic value. Such a renormalization was obtained in our calculations (see Table II). The initial $t_{2g}^4 e_g^2$ configuration [two holes on $d_{xz}^\downarrow, d_{yz}^\downarrow$ orbitals of the t_{2g} set and two on $d_{3z^2-r^2}^\downarrow, d_{x^2-y^2}^\downarrow$ of the e_g set with spin-down (minority) spin projection] results in the self-consistent solution with a magnetic moment of $\mu_{d-Co}=3.16\mu_B$. The total energy of this HS solution is 0.65 eV per formula unit higher than the ground-state LS $t_{2g}^6 e_g^0$ configuration. The unexpected result is that there exists an *intermediate-spin* solution (second line in Table II, magnetic moment value $\mu_{d-Co}=2.11\mu_B$) which is lower in total energy than the HS solution (0.24 eV per formula unit relative to the LS ground state). This solution was obtained when we started from the initial configuration $t_{2g}^5 e_g^1$, where only one electron was transferred from the t_{2g} to e_g states. The final self-consistent configuration is better described as a $t_{2g}^5 \sigma^*$ state with a partially filled σ^* band ($t_{2g}^5 \sigma^*$) with the occupancies of the $a_{3z^2-r^2}^\uparrow$ and $a_{x^2-y^2}^\uparrow$ orbitals equal to 0.84. In a configuration-interaction language used in the cluster calculations, this may be compared to a $d^6 + d^7 \bar{L}$ state, where \bar{L} denotes a hole on the oxygen.

The IS state in our calculations turns out to be metallic (see, however, Sec. III B), and the HS state is semiconduct-

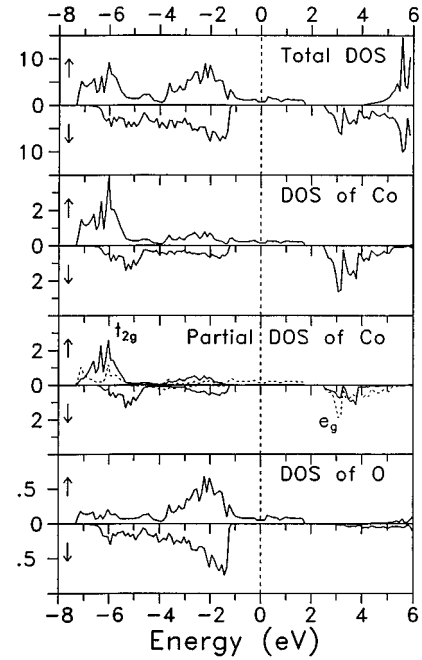


FIG. 2. The total (in states/eV spin cell) and partial (in states/eV spin atom) densities of states obtained in LDA+ U calculations for LaCoO₃ with Co ions in the intermediate-spin state ($t_{2g}^5 \sigma^*$ configuration). The Fermi level is denoted by the vertical dashed line. Arrows corresponds to spin-up and spin-down spin projections. The other notations are the same as in Fig. 1.

ing (Figs. 2 and 3). The reason for this is that the antibonding σ^* band (formed by e_g orbitals) is very broad, and the band splitting is not strong enough to create a gap in the case of an IS state. When the e_g^\uparrow band becomes completely filled (HS state), a small gap between e_g^\uparrow and e_g^\downarrow bands appears.

In Table II the occupation of different orbitals in different configurations is presented. One notices that the actual occupation is different from the formal “chemical” one, and corresponds on the average not to six but rather to seven electrons in the d shell. The reason for this is the strong hybridization of the empty e_g orbitals with oxygen $2p$ orbitals. In the LS ground state every e_g orbital, which is formally empty, actually has an occupancy of about 0.33, resulting in 1.3 additional d electrons above the formal six-electron configuration. In the case of the excited IS state we have a partially filled broad σ^* band, with the total number of e_g electrons increased by 0.85 as compared to the LS, state and the number of t_{2g} electrons 0.92 less than in the LS state, having as a result a practically unchanged total number of d electrons. Therefore, we used the notation $t_{2g}^5 \sigma^*$ in the Table II to prevent a misunderstanding, and in accordance with notation proposed in Ref. 1. One may also say that despite the formal oxidation state Co^{3+} the real configuration, e.g., in the IS state, is a mixture of $t_{2g}^5 e_g^1$ and $t_{2g}^5 e_g^2 \bar{L}$ configurations.

Some other points concerning the results obtained are worth mentioning. As one can see from Fig. 1, the occupied states closest to the Fermi energy in a LS state are mainly formed by oxygen states (note that in Figs. 1–3 the partial densities of states of constituent atoms are given per atom, and there are three oxygen atoms per formula unit). Consequently the final state of XPS for a LS state formally corre-

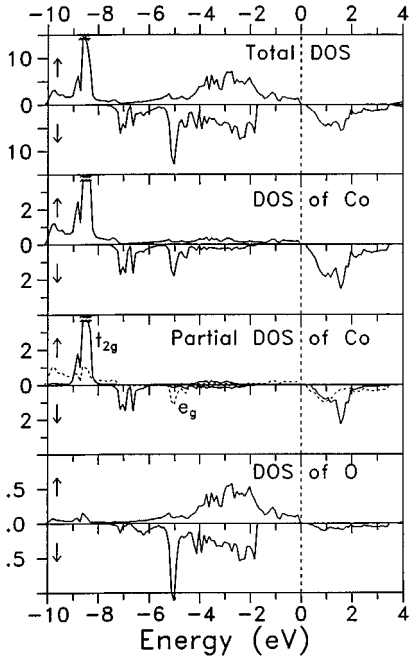


FIG. 3. The total (in states/eV spin cell) and partial (in states/eV spin atom) densities of states obtained in LDA+ U calculations for LaCoO_3 with Co ions in the high-spin state ($t_{2g}^6 e_g^2$ configuration). Notations are the same as in Figs. 1 and 2.

sponds to a $d^6 L$ configuration. At the same time the electronic excitations mostly reside on Co e_g orbitals hybridized with p states of oxygen. However, in the IS case, which in our calculations is metallic (Fig. 2), the states at the Fermi level contain comparable weights of both Co e_g and O p orbitals.

The IS state obtained is fully polarized, which is due to the half-metallic ferromagnetic nature of the solution: the magnetic moment per formula unit is $2\mu_B$, i.e., it corresponds to the spin $S=1$. In that sense the calculation agrees with the ionic picture, in which the IS configuration of Co is $d^6 (t_{2g}^5 e_g^1)$, with $S=1$.

The IS state of LaCoO_3 in our results turned out to be a half-metallic¹⁸ ferromagnet, in which only the electrons of one spin projection are at the Fermi level (the other spin subbands are fully occupied). A ferromagnetic arrangement of the magnetic moments may of course be an artifact of the scheme used. In principle, the LDA+ U method is intended to describe local correlation effects such as a formation of Hubbard gaps and local magnetic moments, which should still be present in the paramagnetic phase. However, technically in the calculations we have to assume a long-range magnetic order in accordance with the translational symmetry of the crystal. The results obtained in such a way indicate whether or not there is a gap, and provide an estimate of the local magnetic moment.

Although the IS state in the calculations turns out to be metallic, the density of states at the Fermi level is very low, $n(E_F)=0.36$ states per eV per one formula unit. This probably indicates that it would not be so difficult to make this state semiconducting; see the discussion below (Sec. III B).

The results presented above show that the first excited configuration lies only 0.24 eV above the ground state with

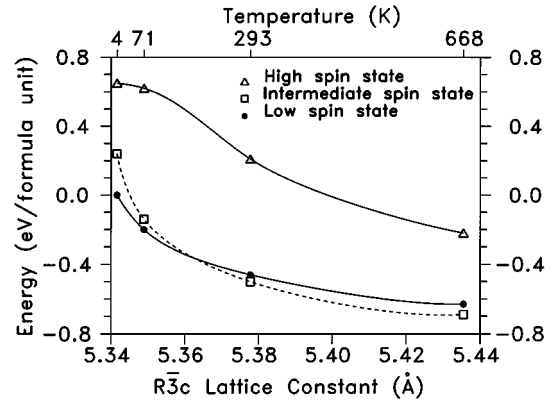


FIG. 4. The total energies for various spin states of LaCoO_3 relative to the energy of the $t_{2g}^6 e_g^0$ state at 4 K vs the $R\bar{3}c$ lattice constant. The corresponding temperatures are also marked.

LS. Experimentally it is established that there is a transition from a LS nonmagnetic state to the magnetic one with increasing temperature. According to Ref. 2, this transition occurs in the vicinity of 90 K. As the closest magnetic state is that with IS (the HS state lies, according to our results, much higher at 0.65 eV), we ascribe the nonmagnetic-magnetic transition in LaCoO_3 to the LS-IS transition.

It is well known (see, e.g., Ref. 1) that Co in the HS state has a larger ionic radius than in the LS one, and the LS-HS transitions are accompanied by an increase of volume. Keeping that in mind, we carried out calculations of the electronic structure of LaCoO_3 for different lattice parameters which can imitate the influence of temperature (via thermal expansion). In Fig. 4 we plot the total energies for various spin states of Co as a function of the lattice parameters relative to the energy of the $t_{2g}^6 e_g^0$ state for the lattice parameter corresponding to 4 K. In this figure the actual lattice parameters used in the calculations are shown on the horizontal axis, together with the corresponding temperature scale (we used the lattice parameters including the lattice constant and rhombohedral angle as a function of the temperature measured in Ref. 3). One sees that with increasing specific volume (or with increasing temperature) the energy of the IS state crosses that of the LS state, which corresponds to the LS-IS transition. In our calculation this crossover occurs at lattice parameters corresponding to 150 K—somewhat larger than the experimental value of about 90 K. Note that the HS state still lies very high in energy even at temperatures above 600 K.

The total energy for all three solutions (LS, IS, and HS) decreases with increasing volume and minima are achieved only for lattice parameters corresponding to high temperature. At this value of the volume the total energy of the IS is slightly lower than the LS. It is well known that equilibrium values of the volume calculated with LSDA are always a few percent less than the experimental volume, because LSDA overestimates cohesion. LDA+ U , on the other hand, underestimates cohesion due to its treating the d states as localized. In both cases the calculated lattice parameters significantly deviate from the experimental values. Goodenough suggested that the magnetic transition in LaCoO_3 is caused by the fact that the crystal-field energy Δ_{cf} is only slightly larger than the intra-atomic (Hund) exchange energy Δ_{ex} .

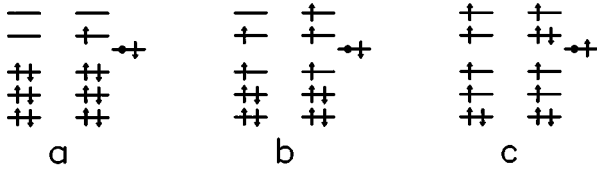


FIG. 5. Schematic representation of various Co $d^6 + d^7 L$ configurations in low- (a), intermediate- (b), and high- (c) spin states. The open circle denotes a hole in the oxygen p shell.

The crystal-field energy is determined by the $3d-2p$ hopping parameters, which strongly depend on crystal volume. Hence if one will perform calculations with lattice parameters corresponding to the calculated equilibrium volume, then the delicate balance between Δ_{cf} and Δ_{ex} will be destroyed. Our results show that for low-temperature lattice parameters Δ_{cf} is larger than Δ_{ex} , but already a small increase in volume (corresponding to increasing the temperature to 150 K) would reverse this ratio.

Thus from the results obtained we conclude that the nonmagnetic-magnetic transition in LaCoO_3 most probably occurs not between LS and HS states, but between *low-* and *intermediate-spin* states. The reason for the stabilization of the IS state may be understood from the following consideration. Different configurations of Co^{3+} (d^6) are illustrated in Fig. 5. Here t_{2g} and e_g are atomic d states split by the crystal field (the splitting $\Delta = 10Dq$). In a purely ionic picture one should expect that, depending on the ratio between Δ and intraatomic exchange interaction J either LS or HS states should be stable (if the energy of the LS state E_{LS} is taken to be zero, then $E_{\text{IS}} = \Delta - J$ and $E_{\text{HS}} = 2\Delta - 6J$, so that the LS state is the ground state for $\Delta > 3J$ and the HS state—if $\Delta < 3J$; the IS state in this scheme would always lie higher). However, as we mentioned in Sec. I, oxides with unusually high valence of transition metals have a tendency to have a d -shell occupancy corresponding to a lower valence, with the extra hole being predominantly located on oxygen (one obtains a configuration $d^7 L$ instead of d^6). In this situation the d - p hybridization is especially strong, and plays a crucial role. These considerations are also supported by our calculations; see Table II.

Especially important is the hybridization with the e_g orbitals. One can show that it is stronger for the IS state than for the HS one: there are more channels of p - e_g hybridization in this case (the most favorable configurations of the type $d^7 L$, admixed to d^6 , are also shown in Fig. 5). In other words, if these configurations ($d^7 L$) are dominant, then the state corresponding to the ground state of the d^7 configuration would have the lowest energy. It is known that for d^7 (Co^{2+}) this is exactly the configuration of Fig. 5(b)—i.e., the one giving a total IS state. This is a possible physical reason why the IS configuration may lie below the HS one, and may become the ground state for an expanded lattice (higher temperatures).

The nonmagnetic-magnetic transition occurring at ~ 90 K, which we now associate with the LS-IS transition, is described reasonably well by our model. The transition temperature obtained in our calculations (~ 150 K) lies not so far from that experimentally observed. In Ref. 2 the relative change of the lattice parameter (Δa) at this transition was fit by the relation (see Ref. 19)

$$\Delta a = \frac{\nu \exp(-E_q/kT)}{1 + \nu \exp(-E_q/kT)}, \quad (8)$$

where E_q is the energy gap (it was taken in Ref. 2 as a fitting parameter), and ν is the degeneracy of the magnetic state. As the high-temperature magnetic ground state was believed to be the HS state in Ref. 2, the degeneracy was taken as $\nu = 15$ [triply degenerated t_{2g} orbital times the spin degeneracy ($2S + 1$) with $S = 2$; see Fig. 5(c)]. In our interpretation the degeneracy will be $\nu = 18$ [triply degenerated t_{2g} orbital times double degeneracy of e_g orbitals times ($2S + 1$) with $S = 1$, see Fig. 5(b)]. Thus the fit of Δa would be as successful with this interpretation as with the one given in Ref. 2, with actually nearly the same value of the energy gap E_q .

The picture of an IS state can also help to resolve one more problem mentioned in Ref. 2: that the correlations between magnetic sites in LaCoO_3 are not antiferromagnetic but (weakly) ferromagnetic. One should expect only antiferromagnetic correlations between *high-spin* Co^{3+} ions in which the e_g shell is half-filled (e_g^2). However, in IS Co, ions have a nominally e_g^1 configuration, and especially if these e_g orbitals are ordered (see discussion below) one can have a ferromagnetic exchange interaction [the well-known example is, e.g., ferromagnetic K_2CuF_4 (Ref. 20)].

B. Possible orbital ordering in LaCoO_3

The concept of the LS-IS transition describes quite reasonably the nonmagnetic-magnetic transition observed in LaCoO_3 . At the same time it was established that the first transition at ~ 90 K leaves this compound semiconducting, whereas our calculated IS has a metallic character of the energy spectrum. Is it possible to overcome this disagreement?

As is clear from Fig. 5(b), the IS state has a strong double degeneracy (e_g^1 configuration). For localized electrons this would be the typical Jahn-Teller situation. In particular for KCuF_3 , it was proposed in Ref. 20 and confirmed by calculations in Ref. 21 that there exists a special kind of orbital and magnetic ordering of d ions in a simple cubic lattice with one electron or hole in a doubly degenerate e_g level. The situation in IS LaCoO_3 is very similar to the case of KCuF_3 (keeping in mind that there exists a permanent rhombohedral distortion, and that there are already two Co ions in an elementary cell in LaCoO_3 , the ‘‘antiferro’’ orbital ordering may be consistent with the existing structural data).

We checked this possibility by repeating the calculations, assuming now that there exists an orbital ordering. The structure of the corresponding ordered IS state was taken as consisting of ferromagnetic planes (001) with an antiferromagnetic coupling between planes. The occupied e_g orbitals were assumed to alternate; as a starting point the orbitals in two sublattices were taken as $d_{x^2-z^2}$ and $d_{y^2-z^2}$; see Fig. 6. To supplement this figure with information about the other d orbitals, let us consider the Co ion in the $t_{2g}^5 e_g^1$ configuration, which has a $d_{y^2-z^2}^\uparrow$ occupied e_g orbital (corresponding site is marked as 1 in Fig. 6). For this state the other three e_g orbitals are empty, and all t_{2g} orbitals are occupied, with the exclusion of d_{yz}^\downarrow . This choice minimizes the Coulomb interaction energy of t_{2g} and e_g electrons. For the neighboring Co ion (site 2 in Fig. 6) the e_g electron is placed in the $d_{x^2-z^2}^\uparrow$

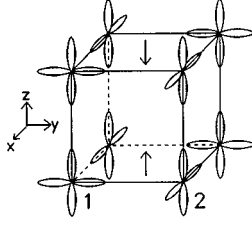


FIG. 6. Spin and orbital ordering in an orbital-ordered intermediate spin state for occupied e_g orbitals. For simplicity the perfect cubic structure of Co ions is shown.

orbital, and the t_{2g} hole is placed in the d_{xz}^\downarrow orbital. Calculations were made for the real rhombohedral crystal structure with lattice parameters corresponding to 71 K. With this state as a starting point the self-consistent calculation was now carried out. The resulting densities of states corresponding to such an orbital-ordered IS state are presented in Fig. 7.

First of all it is necessary to point out that this kind of spin and orbital ordering is stable with respect to the self-consistency iterations, and hence that there exists a solution with such symmetry. The nature of the energy spectrum

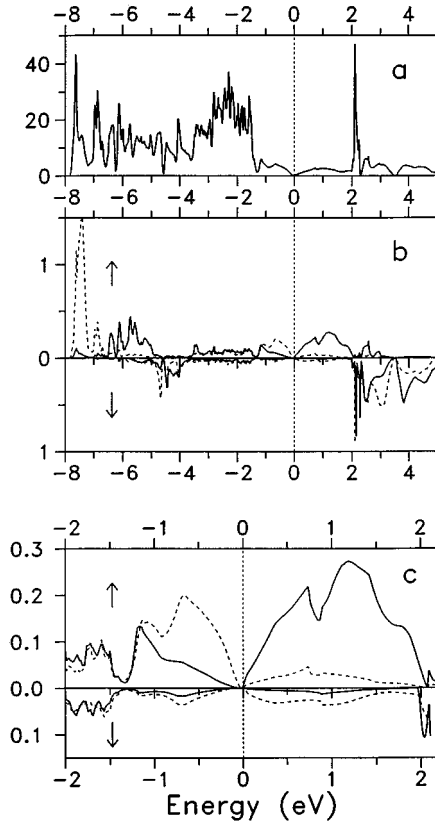


FIG. 7. The total (in states/eV cell) and partial (in states/eV spin atom) densities of states obtained in LDA+ U calculations for LaCoO_3 with Co ions in an orbital-ordered intermediate-spin state. (a) Total density of states (per four formula units and both spins). (b) Partial Co e_g densities of states, e.g., for Co site 1 in Fig. 6: the solid line is for $d_{y^2-z^2}$ states, the dashed line for $d_{3x^2-r^2}$ states. (c) The same as (b) in the vicinity of the Fermi level. The notations are the same in Fig. 2.

turned out to be gapless semiconductinglike. The wide e_g band which crossed the Fermi level in the case of an IS state without orbital order (see Fig. 2) is now split. The top of the valence band is formed (for one sublattice, e.g., for Co site 1) by $d_{y^2-z^2}$ states, and the bottom of the conduction band by $d_{3x^2-r^2}$ states [Figs. 7(b) and 7(c)] hybridized with the oxygen states. As for the t_{2g} densities of states, the character of their energy distribution is practically unchanged in comparison with the case of the IS state without orbital ordering. The spin magnetic moment of Co is found to be $1.87\mu_B$ in this orbitally ordered IS state, and it is less than that without orbital order ($2.1\mu_B$).

When we compare the two IS states with the fixed spin magnetic moment $1.87\mu_B$, the total energy of the orbitally ordered IS state is 0.11 eV lower. The necessity of using a fixed magnetic moment is due to the limitation of the band-structure scheme. The actual magnetic state of LaCoO_3 is known to be paramagnetic (with possible short-range spin or orbital ordering). At the same time, as we already mentioned above, it is necessary to set a long-range magnetic order in the calculations (antiferromagnetic for an orbitally ordered IS state and ferromagnetic for one without orbital order). This long-range magnetic ordering imposed (in addition to the intra-atomic exchange) somehow influences both the local magnetic moment and the total energy. In the case of long-range antiferromagnetic order the value of the magnetic moment is apparently underestimated in comparison with the real paramagnetic state; for the ferromagnetic one it is overestimated. Thus to estimate the relative stability of different phases we compare the energies calculated for the same value of the magnetic moment. Our calculations show that in the case of equal spin values the orbitally ordered IS state is more preferable than the one without orbital order.

One can now interpret the first nonmagnetic-magnetic transition (at about 90 K) as a transition of Co ions from the LS to IS states with a specific orbital ordering of occupied e_g orbitals. Our results show that this transition occurs at temperatures lower than 150 K. Under this transition a magnetic moment on Co sites appears, whereas the material is still nonmetallic. The spin-only value of the *effective* magnetic moment, in the case of an IS state ($S=1$), is $\mu_{\text{eff}}=2.83\mu_B$ —somewhat below the experimental value of $3.1\mu_B-3.4\mu_B$. It will be increased by the orbital contribution, because there is in principle an unquenched moment of t_{2g} electrons for the configuration $t_{2g}^5 e_g^1$ (which, e.g., for Co^{2+} ions increases the value of μ_{eff} by typically $\sim 0.3\mu_B$). We cannot treat this effect numerically because our codes do not include the spin-orbit interaction; however, on physical grounds we expect that this effect should be present. An extra change of μ_{eff} may be due to the very strong $d-p$ hybridization which leads to a large contribution to the total wave function of a state $d^7 L(t_{2g}^5 e_g^2 L)$. In this state the effective moment of the Co ion is that of the high-spin Co^{2+} ($S=3/2$) compensated by the opposite polarization of the oxygen p shell ($S=-\frac{1}{2}$) [note that this picture is supported by calculations (see Table II) where the local Co spin moment is $2.1\mu_B$ and the total spin moment per unit cell is $2\mu_B$]. This fact may significantly change the value of μ_{eff} measured in the susceptibility experiments.

The IS state with a nominal configuration $t_{2g}^5 e_g^1$ may have an orbital ordering because of the doubly degenerate e_g orbitals (the strong Jahn-Teller nature of this configuration). This turned out to be the case in our calculations: the orbitally ordered state may be crudely described as an alternation of the occupied $d_{z^2-x^2}$ and $d_{z^2-y^2}$ orbitals.

According to our calculations, this ordering leads to a splitting of the e_g (σ^*) band, leading practically to the zero-gap situation, with the Fermi level lying in the gap. The second gradual transition to a metallic state (~ 600 K) with an increase of the effective magnetic moment value up to $\mu_{\text{eff}}=4.0\mu_B$ may then be associated with the disappearance of the orbital ordering with increased temperature still within the IS state. This IS state without orbital order is calculated to be a metal with a larger magnetic moment. Our calculations show that the second transition has no relation to the HS state of Co ions because the HS solution still lies high in energy, and if realized would have been a semiconductor state.

IV. CONCLUSION

Calculations of the electronic structure in the LDA+*U* approximation for LaCoO₃ were presented. At 4 K the non-magnetic insulating solution with Co ions in a low-spin state has the lowest total energy. Three excited-state configura-

tions (two of intermediate spin and one of high spin) are also found to be stable, with local magnetic moments on Co sites. The t_{2g} states exhibit narrow bands, while the e_g states form broad bands. With an increasing lattice parameter corresponding to a thermal lattice expansion, two transitions can be expected: the first occurs from the LS state to the IS state, with orbital ordering, which in our calculation is a zero-gap semiconductor. The second transition occurs within the IS state and is connected with a gradual disorder of occupied e_g orbitals. We believe that although many details are not yet clear, the concept of the nonmagnetic-magnetic and semiconductor-metal transitions in LaCoO₃ as connected mainly with intermediate-spin states, is a good candidate to explain the puzzling properties of this interesting material.

ACKNOWLEDGMENTS

We thank Dr. A. Postnikov and R. Potze for helpful discussions. This work was supported by the Netherlands Foundation for Fundamental Research on Matter (FOM), the Netherlands Foundation for Chemical Research (SON), the Netherlands Organization for the advancement of Pure Research (NWO), the Committee for the European Development of Science and Technology (CODEST) program, and the Netherlands NWO special fund for scientists from the former Soviet Union.

*Also at the P. N. Lebedev Physical Institute, Moscow, Russia.

¹J. B. Goodenough, in *Progress in Solid State Chemistry*, edited by H. Reiss (Pergamon, Oxford, 1971), Vol.5; P. M. Raccach and J. B. Goodenough, *Phys. Rev.* **155**, 932 (1967); *J. Appl. Phys.* **39**, 1209 (1968); M. A. Senaris-Rodriguez and J. B. Goodenough, *J. Solid State Chem.* **116**, 224 (1995).

²K. Asai, O. Yokokura, N. Nishimori, H. Chou, J. M. Tranquada, G. Shirane, S. Higuchi, Y. Okajima, and K. Kohn, *Phys. Rev. B* **50**, 3025 (1994).

³G. Thornton, B. C. Tofield, and A. W. Hewat, *J. Solid State Chem.* **61**, 301 (1986).

⁴M. Abbate, J. C. Fuggle, A. Fujimori, L. H. Tjeng, C. T. Chen, R. Potze, G. A. Sawatzky, H. Eisaki and S. Uchida, *Phys. Rev. B* **47**, 16 124 (1993).

⁵J. Zaanen, G. A. Sawatzky, and J. W. Allen, *Phys. Rev. Lett.* **55**, 418 (1985).

⁶J. B. Goodenough, *Mater. Res. Bull.* **6**, 967 (1971); R. H. Potze, G. A. Sawatzky, and M. Abbate, *Phys. Rev. B* **51**, 11 501 (1995).

⁷M. Abbate, R. Potze, G. A. Sawatzky, and A. Fujimori, *Phys. Rev. B* **49**, 7210 (1994).

⁸D. D. Sarma, N. Shanthi, S. R. Barman, N. Hamada, H. Sawada, and K. Terakura, *Phys. Rev. Lett.* **75**, 1126 (1995).

⁹V. I. Anisimov, J. Zaanen, and O. K. Andersen, *Phys. Rev. B* **44**, 943 (1991); V. I. Anisimov, I. V. Solovyev, M. A. Korotin, M.

T. Czyżyk, and G. A. Sawatzky, *ibid.* **48**, 16 929 (1993).

¹⁰V. I. Anisimov, M. A. Korotin, J. Zaanen, and O. K. Andersen, *Phys. Rev. Lett.* **68**, 345 (1992).

¹¹M. A. Korotin, A. V. Postnikov, T. Neuman, G. Borstel, V. I. Anisimov, and M. Methfessel, *Phys. Rev. B* **49**, 6548 (1994).

¹²V. Anisimov and O. Gunnarsson, *Phys. Rev. B* **43**, 7570 (1991).

¹³F. M. F. de Groot, J. C. Fuggle, B. T. Thole, and G. A. Sawatzky, *Phys. Rev. B* **42**, 5459 (1990).

¹⁴M. Methfessel, *Phys. Rev. B* **38**, 1537 (1988); M. Methfessel, C. O. Rodriguez, and O. K. Andersen, *ibid.* **40**, 2009 (1989).

¹⁵A. V. Postnikov, T. Neumann, G. Borstel, and M. Methfessel, *Phys. Rev. B* **48**, 5910 (1993).

¹⁶G. Thornton, F. C. Morrison, S. Parlington, B. C. Tofield, and D. E. Williams, *J. Phys. C* **21**, 2871 (1988).

¹⁷T. Arima, Y. Tokura, and J. B. Torrance, *Phys. Rev. B* **48**, 17 006 (1993).

¹⁸R. A. de Groot, F. M. Mueller, P. G. van Engen, and K. H. J. Buschow, *Phys. Rev. Lett.* **50**, 2024 (1983).

¹⁹D. B. Chesnut, *J. Chem. Phys.* **40**, 405 (1964); R. A. Bari and J. Sivardiere, *Phys. Rev. B* **5**, 4466 (1972).

²⁰K. I. Kugel and D. I. Khomskii, *Zh. Eksp. Teor. Fiz.* **64**, 1429 (1973) [*Sov. Phys. JETP* **37**, 725 (1973)]; *Usp. Fiz. Nauk* **136**, 621 (1982) [*Sov. Phys. Usp.* **25**, 231 (1982)].

²¹A. I. Liechtenstein, V. I. Anisimov, and J. Zaanen, *Phys. Rev. B* **52**, R5467 (1995).